Electrochemical storage of energy in carbon nanotubes and nanostructured carbons

Elzbieta Frackowiak[a], François Béguin[b],*

[a]*Institute of Chemistry and Technical Electrochemistry, Poznan University of Technology, ul. Piotrowo 3, 60-965 Poznan, Poland*
[b]*Centre de Recherche sur la Matière Divisée, CNRS-Université, 1B Rue de la Férollerie, 45071 Orléans Cedex 02, France*

Abstract

Possibilities of electrochemical energy conversion using carbon nanotubes and related materials in various systems, such as lithium batteries, supercapacitors, hydrogen storage, are considered. It is shown that for these applications the electrochemical properties of multiwalled (MWNTs) and single walled (SWNTs) nanotubes are essentially dominated by their mesoporous character. During lithium insertion into nanotubular materials a high irreversible capacity C_{irr} (from 460 to 1080 mAh/g) has been observed after the first cycle with a tendency to further decomposition of electrolyte with cycling. Penetration of solvated lithium ions in the accessible mesopores is at the origin of this phenomenon; an almost linear dependence has been found between the mesopore volume and C_{irr}. Reversible capacity for lithium insertion C_{rev} ranged between 220 and 780 mAh/g; however, a great divergence (hysteresis) between insertion and extraction characteristics was observed independently on the kind of nanotubes and oxygen content. Amount of lithium stored by electrostatic attraction is negligible in comparison to real redox reactions which for thermodynamic reasons present linear variation of potential, especially during deinsertion (pseudocapacitive effects). During positive polarization, i.e., removal of lithium, resistivity of the electrode also gradually increases. Due to the open network of mesopores formed by the nanotubes entanglement, and consequently an easily accessible electrode–electrolyte interface, nanotubular materials are quite adapted for supercapacitor electrodes in various electrolytic solutions. High values of capacitance (80 F/g) have been obtained in 6 M KOH for materials with a surface area of only ca. 430 m^2/g. Capacitance values have been enhanced either by additional oxygenated functionalisation of nanotubes (130 F/g) or by conducting polypyrrole (PPy) electrodeposition where the maximum values reached 170 F/g. The next domain of energy storage in the carbon nanostructures is the accumulation of hydrogen by the electrochemical decomposition of aqueous alkaline medium on a negatively polarized carbon electrode in ambient conditions. For SWNTs only moderate values (below 0.5 wt.% of H$_2$) have been found, while for activated carbons with highly developed surface area of 1500 m^2/g, the amount of reversibly sorbed hydrogen was ca. 2 wt.%, noticeably larger than under dihydrogen pressure (only 0.4 wt.% for the same material at 70 bar and 273 K). The enhancement observed for the activated carbon is interpreted by the formation of nascent hydrogen during water reduction which penetrates easily in the available carbon nanopores. The values obtained by this method are comparable to those of metallic alloys, such as LaNi$_5$ for example.   © 2002 Elsevier Science Ltd. All rights reserved.

Keywords: A. Activated carbon; Carbon nanotubes; D. Electrochemical properties; Gas storage

1. Introduction

At the beginning of this new Millennium, the atmospheric pollution by combustion engines of automotive systems is among the most important industrial problems to be solved. Urgently, it is necessary to start with a world-wide application of environment friendly electric power sources. On the other hand, there is also a big demand for high energy density batteries or fuel cells for portable electronic devices. Actually, most of the devices available on the market in the next 10 years, together with portable systems (mobile phones, lap-tops, camcorders, etc.) should be mainly equipped with lithium-ion, nickel–metal hydride (Ni–MH) batteries or fuel cells [1].

Even if lithium-ion batteries, which combine high power and energy density, appear as the most promising system, there is still a need to improve the electrode materials for achieving the highest capacity while maintaining good electrochemical characteristics. Presently, for the negative electrode, only graphite-based composites are able to fulfil the requirements, i.e., a relatively high reversible capacity at a potential close to metallic lithium and a moderate irreversible capacity.

In the case of Ni–MH batteries, performance is limited by the hydrogen capacity of the anodic material, which does not exceed ca. 1.5 wt.% at room temperature for the most popular LaNi$_5$-based alloys [2]. While weight and cost preclude the use of most of the hydrogen-absorbing alloys for automotive applications, recent works seem to indicate good hydrogen storage capability of nanostructured carbon materials when they are applied for cathodic electrodecomposition of water [3].

The hydrogen–oxygen (air) fuel cells have been developed for many years in spacecraft application, and efforts are underway to provide them to more spread commercial use. They can be used in a wide area of applications, from generating electricity for a utility power plant to running an all-electric or hybrid car to powering a cell phone [4]. It is estimated that using a fuel cell in an all-electric car would be required to store about 3 kg of hydrogen for 500 km driving range. Since the present technologies using high pressure or cryogenic vessels [5] do not allow safe storage and delivery of hydrogen at a reasonable cost, other solutions are strongly required. Recently, an important storage capacity of hydrogen has been claimed for graphite nanofibers and single-wall carbon nanotubes [6].

The last example of modern power sources where carbon materials find an application is the supercapacitor. This kind of cell, characterised by a low energy density, should be mainly used in hybrid systems, providing the high power that a lithium battery is unable to deliver reversibly. In this case, the electrode materials are based on high specific surface area nanostructured carbons.

It turns out that carbons play a key-role in all the storage devices considered above. However, there is still an important search for new or optimised carbons, especially with well-controlled nanostructure and surface functionality, in order to improve the storage capacity and the cycleability of the power supply. Carbon nanotubes, have been carefully considered for all these applications, where their unique morphology (e.g., helical or fishbone arrangement of graphitic layers, presence of a central canal, entanglement, bundles formation, etc.) is expected to be profitable for getting improved performance. Multi-walled nanotubes or nanofilaments (MWNTs) and single-walled nanotubes (SWNTs) have been used for lithium storage [7–12], electrochemical capacitors [13–17], electrochemical hydrogen storage [18,19] and some redox reactions [20,21] applicable for fuel cells.

In this paper, electrochemical applications of nanotubes in energy conversion will be critically discussed and compared to other nanostructured carbons, with some attention for future perspectives. Especially our results on the use of multiwalled nanotubes for lithium insertion and supercapacitors will be presented.

2. Experimental

2.1. Nanotubular materials

Catalytic MWNTs have been synthesized by decomposition of acetylene using cobalt supported on silica at 700 and 900 °C (A/CoSi700, A/CoSi900) or on zeolite at 600 °C (A/CoNaY600) [22–25]. The sample A/CoSi900 was annealed at 2400 °C for 1 h under argon atmosphere, in order to modify its nanostructure. Chemical vapour deposition of propylene at 800 °C within an alumina membrane supplied bamboo-like nanotubes (P/Al800) [26]. In all cases, after the preparation of the nanotubes, the catalyst support or the alumina template were dissolved with 72% hydrofluoric acid, which allowed also to eliminate an important part of cobalt. The samples A/CoSi700 and A/CoSi900 were additionally treated in dilute nitric acid for a further elimination of the free Co particles. After these treatments, the samples were filtered, washed several times with distilled water and dried at 150 °C under vacuum. For a comparison, catalytic Graphite Fibrils™ from Hyperion Catalyst International Inc. (USA), referenced as Hyperion MWNTs, have also been used. They contain 1.2 wt% Fe from the residual catalytic precursor.

The physicochemical parameters of the purified nanotube samples are presented in Table 1. The quantitative determinations of H (hydrogen) and O (oxygen) were performed on the purified materials in the Microanalytical Service of CNRS (Vernaison, France). It must be remarked that a high oxygen content (or surface functionality) is demonstrated by the samples A/CoSi700 and A/CoSi900, that is caused by the post-treatment in nitric acid. This is more remarkable in the case of A/CoSi700 for which transmission electron microscopy showed a surface coating of the nanotubes by pyrolytic carbon. Surface area and micro/mesopore volume were obtained from nitrogen adsorption/desorption isotherms at 77 K (Micromeritics ASAP 2010). Prior to the adsorption experiments, the samples were outgassed (10^{-6} mbar) at 350 °C during 12 h.

From the nanostructural and microtextural characterisations, the catalytic MWNTs appear as a web of curved nanotubes forming often intertwined entanglements [24], while P/Al800 are stiff and of bamboo-like morphology. Mostly the nanotubes tips are opened, except for A/CoNaY600; for the later material, the aromatic carbon layers are remarkably continuous and straight. The material A/CoSi900 has a so-called fishbone morphology with

Table 1
Physicochemical characteristics of the multi-walled nanotubes

Sample Reference	A/CoSi700	A/CoSi900	A/CoSi900 annealed	A/CoNaY600	P/Al800	Hyperion
Outer $\varnothing$ (nm)	10–25	20–50	20–50	10–25	29–40	10–20
Inner $\varnothing$ (nm)	4–8	ca.3	ca.3	3–8	17–32	ca.5
H (wt%)	1.1	0.8	0	0.6	0.5	0.7
O (wt%)	10.8	4.6	0	0.8	<0.3	4.4
S_{BET} (m^2/g)	411	396	191	128	311	290
V_{meso} (cm^3 STP/g)	435	381	242	269	643	609

an ill-defined central canal [24], therefore it is closer to nanofilaments rather than to nanotubes.

In some experiments SWNTs as bucky paper from Rice University (USA) have been used.

2.2. Experimental technique for Li insertion

Electrochemical lithium insertion into the nanotubular carbon host has been performed in a two-electrode Swagelok® cell where a lithium disk was the counter as well as the reference electrode. The carbon electrodes were prepared in the form of pellets with 85 wt.% content of MWNTs, 5 wt.% of acetylene black and 10 wt.% of binding substance (polyvinylidene fluoride, PVDF-Kynar flex 2801, Atochem, France). The electrolytic solution was 1 M LiPF$_6$ dissolved in a mixture (1:1) of ethylene carbonate (EC) and diethylcarbonate (DEC) (Merck). Galvanostatic charge–discharge cycling with a current load of 20 mA/g of carbon has been performed in order to estimate the degree of lithium insertion and extraction, using a multichannel potentiostat/galvanostat MacPile II (Biologic, France). For a better estimation of the kinetics of this process, the galvanostatic intermittent technique (GITT) has been used. Current pulses of 15 mA/g were applied for 2.6 h, that corresponds to an insertion–extraction capacity of ca. 40 mAh/g for each pulse. The evolution of the equilibrium potential between the pulses is measured by allowing the system to relax at open circuit during 20 h.

2.3. Experimental technique for measuring capacitor performance

The above-described nanotubes have been used either in the form of pellets or bucky paper for the assembly of supercapacitors. Two electrodes (positive and negative) of comparable mass ranging from 1 to 20 mg were connected with golden or steel current collectors. Swagelok® type teflon cells were used for the montage of capacitor, including a glassy fibrous paper separator and 6 M KOH or 1 M H$_2$SO$_4$ as an electrolytic solution. Voltammetry and galvanostatic charge–discharge cycling with potential limi-

tation (VMP-Biologic, France) have been used for the evaluation of capacitance values. For a comparison, the electrochemical characteristics have been also investigated by impedance spectroscopy with a Solartron SI 1260 analyzer (Schlumberger) in the frequency range from 100 kHz to 1 mHz at open circuit voltage with 10 mV amplitude.

2.4. Experimental technique for electrochemical hydrogen storage

Storage of hydrogen was carried out by electrolysis of water in 6 M KOH aqueous solution at room temperature and atmospheric pressure, using a three-electrode cell in which disk shape carbon material (10–20 mg) and glassy carbon were the working and counter electrodes, respectively. The reference electrode was Hg/HgO. A VMP multichannel galvanostat/potentiostat (Biologic, France) was used for the galvanostatic cycling of the cell.

3. Lithium storage in carbon nanotubes

The great interest in lithium insertion into different kinds of carbons is connected with the rapid development of lithium-ion batteries in the world market. Intensive research is still focused on the optimisation of anodic carbon materials for getting better performance of this system.

The electrodes of lithium-ion batteries are based on intercalation materials between which lithium ions are transferred through the electrolytic medium during charge and discharge [27]. The cathodic (positive electrode) materials are lamellar oxides such as LiCoO$_2$, LiNiO$_2$ or LiMnO$_2$, represented by the general formula Li$_y$MO$_2$ ($y \approx$ 1), while carbon (more generally graphite) is used for the negative electrode (anode). The following equations represent the redox reactions in the cell:

$$6C + xLi^+ + xe^- \Leftrightarrow Li_xC_6$$

$$Li_yMO_2 \Leftrightarrow Li_{y-x}MO_2 + xLi^+ + xe^-$$
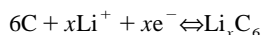
Using a graphite anode, such a battery operates at almost constant voltage of about 3.5 V during discharge [28], that makes this system very attractive for its high energy density. In the case of graphite, lithium penetrates between the graphene layers through an intercalation process with charge transfer to carbon. The successive formation of stages 3, 2 and 1 derivatives [29–31] is demonstrated by well-defined plateaus at constant potential on the galvanostatic curves (Fig. 1), reaching the composition LiC_6 at saturation. It is remarkable for graphite that insertion–extraction proceeds very close to the potential of metallic lithium, allowing the lithium-ion battery to discharge at high and almost constant value of voltage. Nevertheless, in Fig. 1 it must be pointed out that a part of lithium, being involved in the so-called solid electrolyte interphase (SEI), as Li_2CO_3 for example, is not recovered in the electrolyte during deintercalation (oxidation) giving rise to a noticeable irreversible capacity. For the following presentation, the curve shown in Fig. 1 will represent a kind of reference which advantageous characteristics should be at least reached. An optimal carbon material for lithium-ion batteries should have a higher reversible capacity than graphite, while keeping a small irreversible capacity and its main part of discharge (oxidation) below 0.5 V versus Li. During the last years, many efforts have been devoted to develop electrodes based on the use of hard carbons, because of the high reversible capacity which can be reached with some of these materials, without the inconvenience of exfoliation during insertion–deinsertion processes. However the main drawbacks are an important irreversible capacity and a varying voltage during lithium deinsertion [27]. A developed active surface area (ASA) might be essentially responsible for the irreversible capaci-
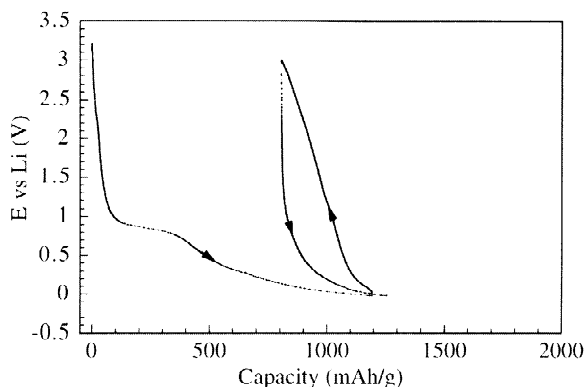

Fig. 2. Galvanostatic insertion–extraction of lithium into A/CoSi900 nanotubes. Current load of 20 mA/g.

ty, at least for microporous carbons, and post-treatments tending to reduce ASA are profitable for SEI decrease [32].

Among many carbons, nanotubes and nanofilaments were also investigated for lithium storage by a few groups [7–12]. A significant reversible capacity has been found, up to 780 mAh/g for A/CoSi700 and 1000 mAh/g for ball-milled SWNTs [11], however with some drawbacks. Fig. 2 presents a galvanostatic charge–discharge curve [33] that is quite typical for all this family of materials, including SWNTs, MWNTs and nanofilaments. The lack of plateau during lithium deinsertion (oxidation) precludes any application of these electrodes in lithium-ion batteries. On the other hand, in all cases the irreversible capacity, C_{irr}, is extremely high. This contribution which represents
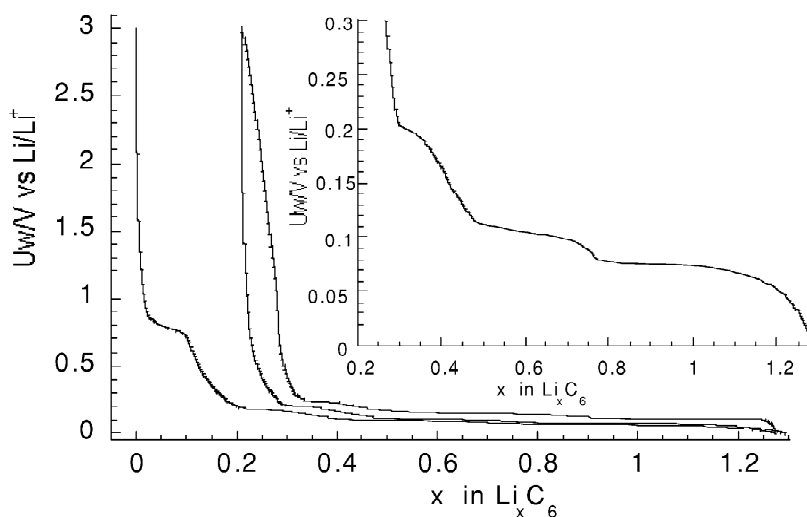

Fig. 1. Galvanostatic intercalation–deintercalation of lithium in graphite using a two electrode lithium–graphite cell. Inset: the part of the curve close to 0 V versus Li is enlarged showing clearly the stage transitions at constant potential.

the fraction of lithium irreversibly trapped requires an additional mass of cathodic material. Among many factors, it is assumed that the SEI formation mainly contributes to the value of C_{irr}. In the case of graphitic type or microporous carbons, a linear dependence is often noted between C_{irr} and the BET specific surface area [34]. For a wide variety of nanotubular materials it is now well established that such a relationship is not applicable, proving that carbons which are essentially mesoporous present a different behavior, as for example chars from nanocomposites [33,35].

Therefore, we have plotted C_{irr} measured after the first discharge–charge cycling versus the mesopore volume for the different types of nanotubes listed above (Fig. 3). The almost perfect proportionality indicates that the central canal and/or mesopores formed by nanotubes entanglement are surely favouring the SEI formation, by allowing an easy access of the voluminous solvated lithium cations to the active surface where they can be transformed into decomposition products. Moreover, during subsequent cycling of electrodes from nanotubes, an additional passivation layer is formed, as it is well demonstrated by the continuous increase of C_{irr} in Fig. 4. This means that, in the case of carbons with open mesopores, solvated ions can still penetrate to the interior of the electrode where they can be further decomposed. Simultaneously, the reversible capacity also diminishes (Fig. 4), and the capacity loss is estimated as ca. 30% after 10 cycles. Definitively, carbons
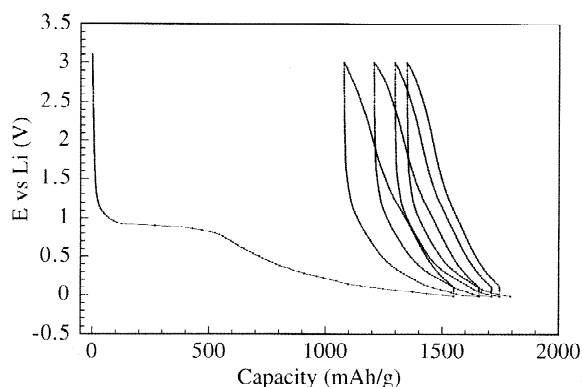

Fig. 4. Lithium insertion/extraction for P/Al800 nanotubes during a few cycles. Current load of 20 mA/g.

with small micropores are required for limiting the extent of SEI formation and the associated fading of reversible capacity during cycling.

For all types of nanotubular materials, a high divergence is observed between the values of insertion and extraction potentials [7–12], that is commonly called hysteresis. It is interesting to compare the galvanostatic characteristics of as-received A/CoSi900 (Fig. 2) and of the same material after a graphitization treatment at 2400 °C (Fig. 5) [8]. Though the two materials keep a significant value of
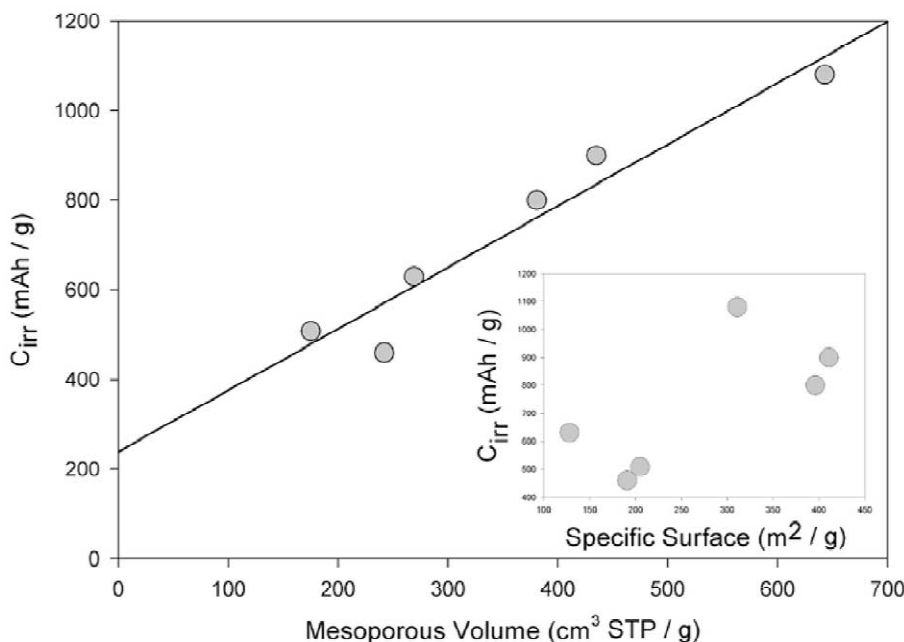

Fig. 3. Dependence of irreversible capacity C_{irr} versus mesopore volume for different types of nanotubes. The inset shows the absence of proportionality between C_{irr} and the specific surface area in the case of a mesoporous material.
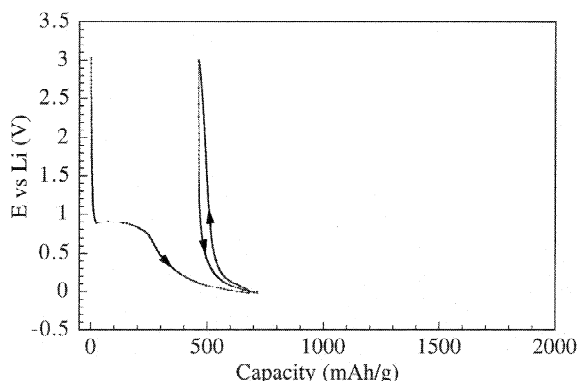
Fig. 5. Lithium insertion–extraction into A/CoSi900 nanotubes treated at 2400 °C. Current load of 20 mA/g.

irreversible capacity, because of their important mesopore volume, they mainly differ for the shape of the oxidation curve. The presence of hysteresis is the most pronounced for pristine A/CoSi900 with a high oxygen content (ca. 5 wt%) introduced during the purification process by nitric acid [8,33]. Higher convex character of the oxidation curve is even demonstrated by A/CoSi700 which contains ca. 11 wt% of oxygen. Among other effects, convexity of the curves during deinsertion might be partly attributable to quasi-reversible interactions between oxygenated surface groups and lithium, such as, for example, COO^-Li^+.

The oxidation process can be arbitrarily divided into two parts, below and above ca. 0.5 V versus Li, respectively. The low potential part at almost constant potential is rather related with lithium intercalated between graphitic type layers. This interpretation is supported by Fig. 5 showing that graphitized A/CoSi900, with larger graphitic type domains than the pristine material, presents a larger value of reversible capacity below 0.5 V versus Li, i.e., 150 mAh/g against 110 mAh/g for as-received A/CoSi900 (Fig. 2). The almost linear dependence of potential noted in Fig. 2 above ca. 0.5 V versus Li during the galvanostatic deinsertion cannot be explained by electrostatic discharging of an electrical double layer. Indeed, for nanotubes the amount of lithium trapped through this electrostatic effect does not exceed 5–10% of the total capacity. The high value of reversible capacity for this material is mainly due to a redox insertion–reduction process with charge transfer between carbon and Li_n^+ clusters formed in the mesopores, i.e., either in the meniscus between entangled nanotubes or in the central canal. Hence, the linear increase of oxidation potential above ca. 0.5 V versus Li indicates a continuous change of free enthalpy during Li_xC_6 decomposition, i.e., the progressive evacuation of lithium from sites where the interactions with the carbon network are continuously changing. This phenomenon called pseudocapacitive effect, originated with the existence of mesopores, is the only reason for hysteresis as well as high lithium capacity. It must be pointed out that the micropore volume, which

was found to be negligible from the nitrogen adsorption measurements, does not contribute markedly to the pseudocapacitive behavior of the nanotubular materials. In the case of annealed A/CoSi900, which keeps quite a high value of accessible mesopore volume despite the graphitization treatment, it might be assumed that the small value of capacity related with oxidation (Fig. 5), above ca. 0.5 V, is essentially due to the effect of the electrical double layer.

Additionally, as a consequence of a huge amount of electrically insulating SEI, the resistance of the cells changes rapidly depending on the degree of lithium insertion. The variation of the resistive character of nanotubes electrode has been perfectly confirmed by galvanostatic intermittent titration technique (GITT), submitting the cells alternatively to weak discharge or charge pulses and to open circuit periods (relaxation). Fully lithiated nanotubes represent a well-conducting material due to the charge transfer to carbon, on the other hand delithiated materials are significantly less conductive than pristine (Fig. 6). A careful observation of the subsequent electrode responses for such pulses allowed to distinguish between resistive and diffusive polarisation especially during lithium deinsertion, that gives a general idea about the complexity of the total process. This relaxation curve also shows how much this system is far from the equilibrium conditions, especially during lithium extraction. It is clearly seen that, even neglecting the resistive and diffusion part, a significant difference of ca. 1 V between insertion and extraction curves still remains and this can be only explained by thermodynamic reasons, that matches well with a pseudocapacitive behavior.

^{7}Li NMR supplied some complementary information about the mechanism of lithium insertion into the carbon nanotubes after annealing [8]. The observed values of Knight shift are relatively small, from 5 to 20 ppm. It confirms the iono-covalent character of stored lithium and proves the lack of pseudometallic aggregates which are
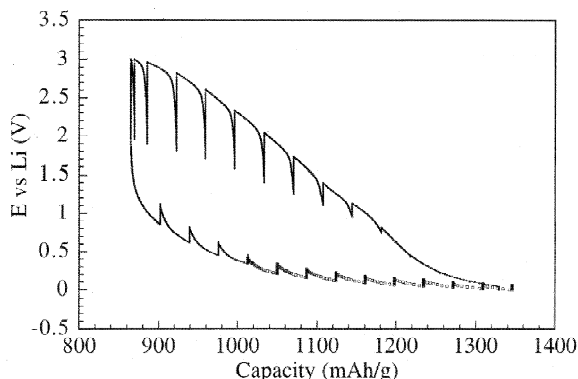

Fig. 6. Galvanostatic intermittent titration technique (GITT) for A/CoSi900 nanotubes. Current pulses of 15 mA/g. Relaxation time 20 h.

observed in the case of microporous carbon with a 60 ppm shift [36]. The obtained results fit well with the negligible values found for the micropore volume of nanotubes.

Milling has been considered as a method for some improvement of electrochemical performance of nanotubular materials [11]. Typically for any kind of carbon, a milling process is the source of particles breaking and forming free radicals. Hence, the conditions of the milling technique (time, type, atmosphere) and the possible saturation of these bonds are extremely important [37]. It was proved that only 10 min milling preserves a major phase containing SWNTs, whereas the proportion of disordered carbon together with the formation of amorphous carbon increases after 20 min. From the electrochemical data, it has been found that for short time ball-milled SWNTs [11] the irreversible capacity decreases from $x = 4$ to $x = 1$, and the reversible saturation Li composition increases from $Li_{1.7}C_6$ to $Li_{2.7}C_6$. The physico-chemical characterisation of the milled nanotubes confirmed a disorder induced within the bundles and a fragmentation of the SWNTs. It seems that the milling process causes a different arrangement of nanotubes and morphology, with the appearance of a more irregular structure, i.e., a 1–10-μm coating of densely packed particles on the surface of nanotubes. Hence, this increase in packing of the nanotubular material, and probably the decrease of mesopore volume, is mainly responsible for the reduction of C_{irr}. The more pronounced C_{rev} after milling could be related with the increase of electrochemically available sites for lithium storage. A large voltage hysteresis between discharge and charge cycle is observed for all the samples independently of milling, that proves the same mechanism of lithium storage for both cases, with a multi-site occupation in the nanotubes ropes and different lithium–carbon interactions.

As long as post-treatment conditions will not be found for curing the lack of voltage plateau during lithium extraction (hysteresis) and the huge irreversible capacity, a practical application of nanotubes for lithium storage in lithium-ion batteries is precluded. Nevertheless the presence of a well-developed network of open mesopores for the nanotubular-like materials and the easy diffusion to the active surface demonstrated by solvated ions suggests promising properties of nanotube-based electrodes in electrochemical capacitors.

4. Supercapacitors from nanotubular materials

In the electrochemical capacitors, the electrical charge is accumulated in the double layer mainly by electrostatic forces [38]. The stored energy is based on the separation of charged species across the electrode–solution interface. The electrochemical capacitor contains one positive electrode with electron deficiency and the second one with electron excess (negative). The amount of electrical energy W accumulated in such a capacitor is proportional to

capacitance C and voltage U ($W = 1/2CU^2$). The main advantage of this storage device is the ability of a high dynamic of charge propagation, that allows a rapid withdrawing of energy (electrodes do not undergo phase transformations as in accumulators). Such a resulting high power can be adapted in the hybrid energy sources for electrical vehicles, computers, UPS and pulse laser technique.

The electrochemical capacitors based on carbon electrodes are of two types, i.e., electrical double-layer capacitors where only a pure electrostatic attraction between ions and the charged surface of the electrodes takes place, and supercapacitors based additionally on faradaic pseudocapacitance reactions [38]. The values of capacitance are strictly connected with the nature and surface of the electrode–electrolyte interface. Generally the more developed the specific surface area of carbon, the higher the ability for charges accumulation ($C = \varepsilon S/d$, ε is permittivity of the electrolyte, S is surface area of the electrode–electrolyte interface, d is distance between the polarised carbon surface and the maximum charge density of solvated ions). However, this surface must be electrochemically accessible for the ions, hence, apart of high values of specific surface area determined by microporosity, the presence of mesopores is essential for ions transportation. The dimensions of pores should be adapted to the size of solvated anions and cations that is crucial for a high performance of capacitor. Indeed, a quick transportation of ions in the bulk of electrodes can fulfil the so-called frequency response, i.e., the ability for energy extraction at higher frequencies (e.g., 1 Hz). The application of nanotubes for this function of a capacitor [13] seems to be promising due to their unique network of mesopores formed both by the entanglement of nanotubes and the central canal. Finally, the surface wettability should not also be neglected for an optimised performance of capacitors.

4.1. Capacitance properties of nanotubes

The electrochemical characteristics of supercapacitors built from MWNTs have been investigated and correlated with the microtexture and elemental composition of the materials [14–16]. The capacitance (per gram of nanotubular material) was calculated mainly from the galvanostatic discharge and voltammetry characteristics at 2 mV/s scan rate (Table 2). In 6 M KOH aqueous electrolyte, most of the nanotube based capacitors give a regular box-like shape of voltammograms. The higher the BET specific surface area and oxygen content of the nanotubes, the higher values of capacitance. Capacitance values as high as 80 F/g of carbon nanotubes have been found, even if the specific surface area of the materials reaches only a moderate value of maximum 450 m^2/g [14]. The functionalisation of A/CoSi700 by hot nitric acid (80 °C for 1 h) increases additionally the capacitance value to 130 F/g,

Table 2
Values of capacitance (F/g) for different nanotubular materials in 6 M KOH

Sample	ACo/Si700	A/CoSi900	A/CoNaY600	P/Al800	Hyperion	SWNT	SWNT 1650 °C
(F/g)	80	62	4	36	14	40	18

and a reversible ill-defined redox peak due to an oxygenated surface functionality is noted at ca. 0.2 V in the voltammetry curve (Fig. 7). However, the increase of capacitance is not stable with cycling typical for this type of pseudocapacitance due to the presence of surface groups. Another kind of effect not strictly connected with the charging of an electrical double layer has been demonstrated by Hyperion™ catalytically grown nanotubes. Depending on the electrolytic solution, the capacitance reached different values (14 F/g in 6 M KOH and 78 F/g in 1 M H_2SO_4), clearly showing that redox pseudocapacitive reactions take part due to the dissolution of iron impurities (1.2 wt%) [16].

SWNTs (Rice University) have been also investigated for comparison and they supplied a value of 40 F/g (Fig. 8). After their annealing at 1650 °C, capacitance diminishes to 18 F/g due to a better arrangement of the tubes in the bundles, that hinders the diffusion of solvated ions towards the active surface.

Generally for activated carbons there is almost a linear relationship between the specific surface area and capacitance. In the case of MWNTs and SWNTs, the specific surface area is moderate, ca. 400 m^2/g, and microporosity very limited. Hence, the ability for charges accumulation in the electrode–electrolyte interface strongly depends on the ions accessibility to the outer walls and central canal of nanotubes, and on the total number of defects. On the other

hand, the presence of a dense pyrolytic carbon outer layer is able to aggravate ions storage. However, if the micropores of pyrolytic carbon covering the nanotubes are enough large to be penetrated by the solvated ions, they can play a great role in the charging of the double layer. Additionally, the values of capacitance are enhanced if the tips of nanotubes are open, that seems to be a proof of accumulation of charges in the central canal. However if the canal is too large, i.e., over the diameter of a few solvated ions, it does not play any positive role for charging the double layer. It was the case of template nanotubes P/Al800, obtained with different times of deposition, where the values of capacitance varied from 5 to 40 F/g depending on the diameter of central canal (100 and 10 nm, respectively). In the case of a very large canal and only a few concentric graphitic layers which form the nanotube wall, the electrochemically active electrode–electrolyte interface is very small. Hence, optimized carbon nanotubes for a supercapacitor should possess a great number of graphene layers, an open central canal with diameter below 5 nm (taking into account the size of a few solvated ions) and an interconnected entanglement. All the defects and roughness of walls are very favourable for charging the electrical double layer. Optimal would be additional stable pseudoeffects which could significantly enhance the values of capacitance, e.g., conducting polymers or other electroactive species deposited on the nanotubes.

4.2. Capacitors from nanocomposites

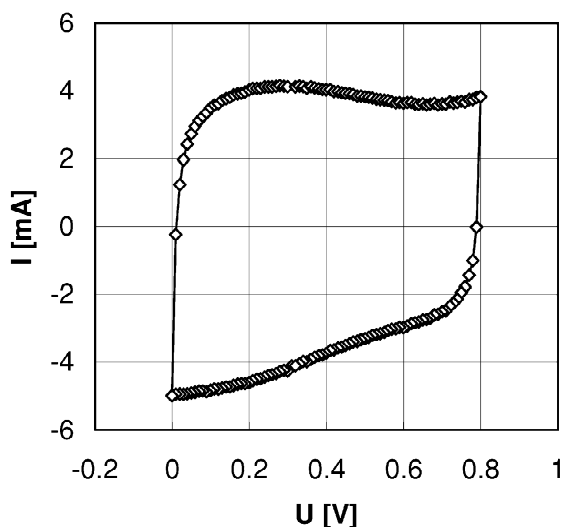A novel type of composite electrodes based on MWNTs

Fig. 7. Voltammetry characteristics (10 mV/s) of a supercapacitor built from A/CoSi700 modified by nitric acid. Electrolyte, 6 M KOH.
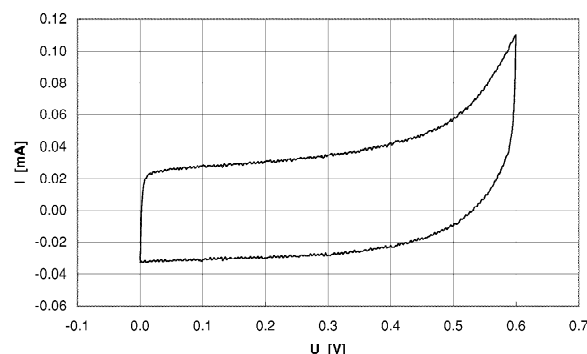

Fig. 8. Voltammetry characteristics (2 mV/s) of a supercapacitor built from SWNTs operating in 6 M KOH. Mass of each electrode, 1 mg.

with deposited polypyrrole (PPy) has been used for the assembly of supercapacitors. Chemical and electrochemical polymerisation of pyrrole has been considered in order to get a homogeneous layer of PPy on the nanotubular materials. The homogeneity and the thickness of the PPy layer in the composite material were estimated by scanning electron microscopy. Chemical deposition of PPy on nanotubes or fibres supplied a non-homogeneous type of deposit with a tendency to form some aggregates. On the other hand, the application of the electrochemical method gave a very unique deposit of a homogeneous PPy film with a good conductivity. The SEM micrograph of the nanotubes A/CoNaY600 with electrodeposited PPy (Fig. 9) shows a homogeneous coating; by comparison with the diameter of the pristine material, the film thickness is equal to 5 nm.

Cyclic voltammetry with a scan rate of potential from 1 to 10 mV/s and galvanostatic charge–discharge cycling from 0 to 0.6 V or higher voltage limitation (0.8, 1.0 or 1.2 V) were performed to estimate the values of capacitance. The effect of PPy on the capacitance properties of A/Co700 measured by voltammetry is shown in Fig. 10. The square shape of the voltammogram for this nanocomposite (Fig. 10) would suggest a pure electrostatic attraction, even if pure PPy usually gives more irregular characteristics, confirming a good synergy between PPy and MWNTs. This kind of capacitive behavior is confirmed by the linear discharge on the galvanostatic curve (Fig. 11).

Electrochemical impedance spectroscopy, as a powerful technique for the investigation of the capacitive behavior
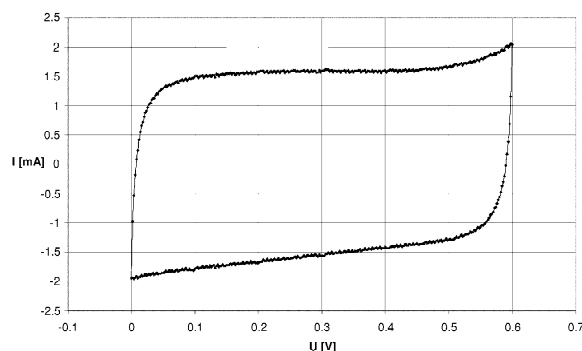
Fig. 10. Voltammetry characteristics (2 mV/s) of a capacitor built from carbon nanotubes A/CoSi700 modified by electrodeposited PPy. Electrolyte, 1 M H_2SO_4. Mass of each electrode, 11.6 mg.

of electrochemical cells, has been also used to check the ability of the novel composite carbon materials to store electrical energy. An example of the Nyquist plots for the material A/CoNaY600 and for the nanocomposite A/CoNaY600+PPy is shown in Fig. 12. In the case of the PPy composite, the diffusion part is remarkable (Warburg part of the impedance spectrum) what could be a sign for some diffusive limitations. Generally, all the impedance spectra of the investigated materials exhibit a capacitive behaviour in the low frequency range with a quite vertical dependence of the imaginary part versus the real impedance part. In the high frequency region on the Nyquist plots of all the samples we could also notice a small time constant which is related to the electrical charge transfer at
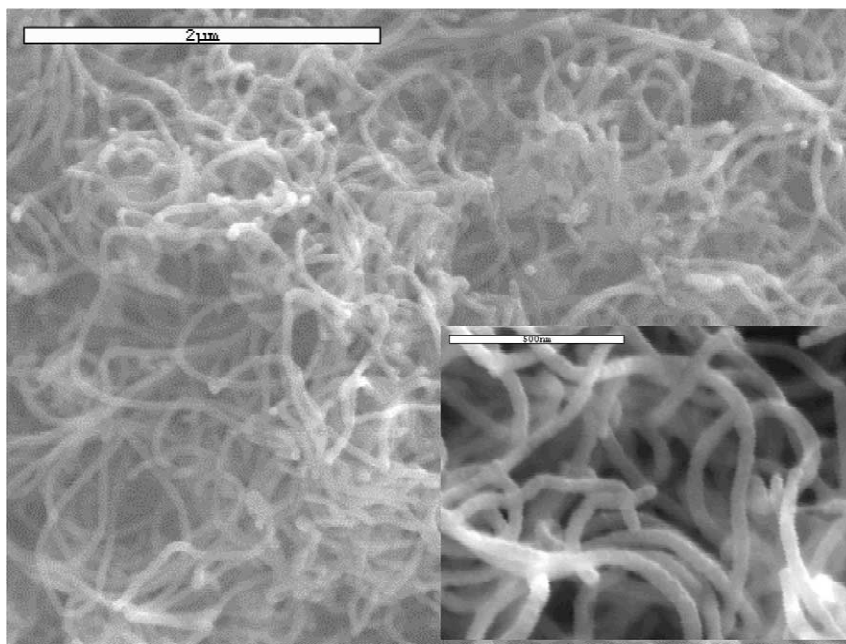
Fig. 9. SEM micrograph showing a homogeneous population of carbon nanotubes A/CoNaY600 coated with electrodeposited polypyrrole.
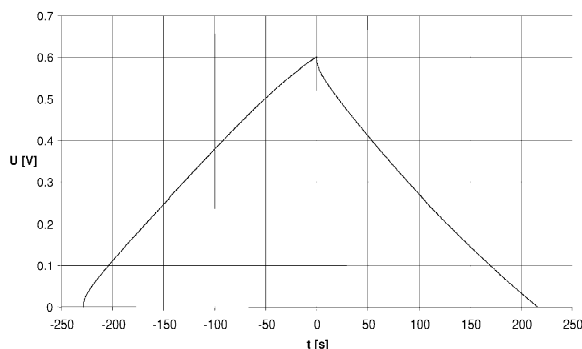
Fig. 11. Galvanostatic charge–discharge of a capacitor built from carbon nanotubes A/CoSi700 modified by electrodeposited PPy. Mass of each electrode, 11.6 mg. Current of 2 mA.

the carbon materials. The capacitance of the cells was evaluated from the low-frequency data of the spectra and a good correlation has been found between all the techniques even if the values given by impedance spectroscopy are lower, that is typical for this method (an alternative current penetrates into the pores with hindrance).

Galvanostatic discharge seems to be the most reliable method for getting the values of capacitance in F/g of active nanotubular material for all the investigated samples (Table 3). From the analysis of these data, we can see that the nanotubular materials with electrochemically deposited polypyrrole give significantly higher values of capacitance than the pristine nanotubes. A maximum value of ca. 170 F/g has been obtained for MWNTs prepared at 600 °C and modified by a PPy layer of 5 nm. This is about twice higher than the value given by the pristine nanotubes, ca. 80 F/g, that is a proof of a synergy effect between nanotubes and PPy. It seems that the open entangled web
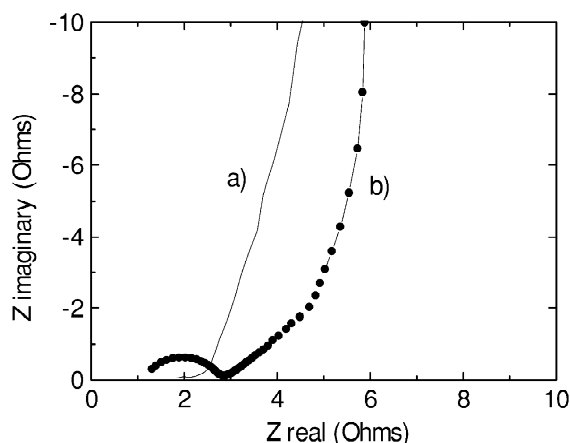

Fig. 12. Impedance Nyquist plot of supercapacitors built: (a) from carbon nanotubes A/CoNaY600 (mass of each electrode, 7.0 mg); (b) from the nanocomposite A/CoNaY600 + PPy (mass of each electrode, 11.3 mg).

Table 3
Capacitance values (F/g) of the nanotubular materials in acidic medium (1 M H_2SO_4) without and with PPY

Kind of nanotubes	C (F/g) without PPy	C (F/g) with PPy
A/CoSi700	65	141
Hyperion™	78	146
P/Al800 (inner $\varnothing$ 100 nm)	5	123
A/CoNaY600	50	163

of the nanotubular composite allows to form a volumetric electrochemical capacitor where the charge has a three-dimensional distribution. It is remarkable that pristine template nanotubes P/Al800 with a large central canal and an extremely low specific surface area (below 50 m^2/g) demonstrate negligible values of capacitance (5 F/g). In this case mainly electrodeposited PPy is responsible for the high value close to 130 F/g of nanotubular composite material. Taking into account the large diameter of central canal for these tubes, ca. 100–200 nm, it might be expected that a thin PPy film also covers the inner core which still remains accessible for the electrolyte. The high value of capacitance compared to pristine P/Al800 originates from inner and outer coating of the nanotubes.

Due to the open network of mesopores in the nanotube/ PPy composites, the bulk of the thin PPy layer is fully involved for quick pseudofaradaic processes, that is the reason for the high values of capacitance. Taking into account that some of the investigated capacitors have been cycled over 2000 cycles, with a charge loss which never exceeded 20%, nanotubes coating by a thin layer of conductive PPy seems to be an efficient process for the realisation of long durability materials. Hence, this new kind of nanocomposites, easily manufactured at reasonable costs, presents very promising perspectives for future capacitor application of nanotubes.

5. Electrochemical storage of hydrogen

Among all the trials for application of nanotubes in energy conversion, especially storage of hydrogen supplied a lot of controversy and discrepancy in experimental and theoretical results taking into account the amount of sorbed gas, forces and sites for its accumulation [39]. Already about 20 years ago, Carpetis and Peschka reported relatively important adsorption of ca. 3–6 g of hydrogen for 100 g of high surface area activated carbons at 78 K and up to 40 bar of hydrogen pressure [40]. Later, it was shown by Agarwal et al. for similar experimental conditions that the amount of hydrogen adsorbed increased with the surface acidity of the activated carbons [41]. More recently, it has been claimed that a large amount of hydrogen is sorbed in graphite nanofibers or nanotubes at room temperature [42]. The high values indicated for

graphite nanofibers were never confirmed, and a careful work by Ahn et al. demonstrated that, after admitting a hydrogen pressure of 180 bar at 300 K, the absolute level of hydrogen desorption measured from these materials was typically close to 0.5 wt.%, comparable to other forms of carbon such as Saran coke [43]. After the first claim that hydrogen could be inserted at room temperature in the canal of single-wall carbon nanotubes (SWNTs) [42], there is not a clear statement on the amount which could be sorbed. Experimental data show a wide range of values from 0.1 to 10 wt.% of H_2 depending on the purity of material and sorption conditions. Theoretical computations indicate that H_2 molecules are rather sorbed in the canal and that the storage capacity increases linearly with the tube diameter, exceeding 14 wt.%, i.e., 160 kg H_2/m^3 [44]. Experimentally, a hydrogen storage capacity of 4.2 wt.% has been claimed to be achieved at 300 K under a high pressure of 100 bar for a sample of single-wall nanotubes with a large mean diameter of about 1.85 nm; about 80% of the adsorbed hydrogen could be released under ambient pressure at room temperature [45]. In a recent paper, considering not only SWNTs or MWNTs but also vapor-grown carbon fibers, carbon filaments, activated carbon, Tibbetts et al. showed that the largest sorption observed is less than 0.1 wt.% hydrogen at room temperature and 3.5 MPa [46].

Generally for physical sorption of hydrogen, a pressure of 100 bars or low temperature ca. 77 K is needed. On the other hand, in all the cases, there is only a partial release at room temperature, which tends to demonstrate that a part of hydrogen is in the state of chemisorption.

Due to a good electronic conductivity of carbons, electrodecomposition of aqueous alkaline solution on a cathodically polarised electrode from these materials seems to be an alternative and elegant method for reversibly storing hydrogen in the microtexture of carbon at ambient pressure and temperature. The amount of reversibly accumulated hydrogen is easily estimated from anodic charge. Such a process has been studied by Nützenadel et al. for carbon samples containing nanotubes [47]. For a material based on single-wall nanotubes, they noticed a discharge capacity which corresponds to 0.39 wt.% of hydrogen, claiming that no other form of carbon absorbs comparable amounts of hydrogen [47]. In the case of a multiwalled carbon nanotube–nickel composite electrode, a reversible capacity of ca. 0.7 wt.% has been found [48]. Even bigger adsorption values up to about 2.9 wt.% were claimed after screening a number of single-wall carbon nanotubes samples with different degrees of purity [49,50]. However, if one looks carefully at the data published in Ref. [47], there is no systematic relationship between the indicated purity and the maximum discharge capacity. This suggests that single-wall carbon nanotubes are probably not responsible for the values of sorption observed. Indeed, whatever the method of preparation, besides nanotubes the materials always contain other forms of carbon, mainly strongly disordered. On the other hand, to give a precise statement on the purity of SWNTs purity based on transmission electron microscopy or scanning electron microscopy is impossible.

These considerations led us to the conclusion that electrodecomposition of water is probably more efficient on other forms of carbon than nanotubes. On the other hand, the use of nanotubular materials for this application is quite doubtful because of the cost, limited scale production and uncertain purity. Therefore, we decided to check hydrogen adsorption by electrolysis of water on an activated carbon electrode [3]. We selected activated carbon fabrics, because they can be readily available in quite large amounts and no binding substance or enhancing conductivity additive is necessary for the manufacture of the electrode. The amount of hydrogen released after an electrochemical load ranges from ca. 1.5 to 2 wt.% and is about five times higher than that which is adsorbed under a gas pressure of 70 bar at 273 K on the same material [3]. A moderate oxidation of the carbon fabric, with a total surface functionality of ca. 3.5 meq/g, slightly improves the hydrogen storage by about 0.2 wt.% [3]. On the other hand, a strong oxidation of carbon by NaOCl was very harmful, increasing the resistivity of the material. The enhancement of reversible capacity through water reduction is interpreted by the formation of nascent hydrogen which penetrates easily in the carbon nanostructure, rather than being trapped by the surface functional groups. The electrochemical process of insertion and release of hydrogen was repeated many times showing its reversibility without significant aggravation.

These values are comparable to the reversible hydrogen capacity of some disordered multi-element alloys used in nickel–metal hydride systems at room temperature [51]. Finally, it must be pointed out that a number of SWNTs materials have been investigated by the same electrochemical technique, and the reversible hydrogen storage capacity never exceeded 0.5 wt% [52]. This value is in quite good agreement with a number of recent publications demonstrating that dihydrogen storage capacity of SWNTs under a high pressure at room temperature is negligible [46]. Therefore, nanostructured activated carbons, due their low cost and easy availability in large amount, are probably the unique kind of carbon substrate which should be considered in the future for hydrogen storage, provided that electrochemical conditions will be used. Additionally, to associate in a unique step the hydrogen production by water electrolysis and its simultaneous storage in a carbon substrate is quite attractive from the point of view of energy efficiency.

6. Conclusion

The mesoporous character of carbon nanotubes plays a dominant role in their electrochemical properties. Com-

pared to conventional carbon materials, carbon nanotubes have higher rate of electron transfer. Their entangled network and central canal are at the origin of pseudo-capacitive effects, allowing an easy access of the ions to the electrode/electrolyte interface.

Relatively high values for lithium insertion degree up to $x = 2.1$ (in Li_xC_6) but with a significant hysteresis confirm that lithium insertion follows faradaic redox reactions but with a capacitive character (so-called pseudoeffects). The lack of voltage plateau during lithium deinsertion, i.e., the continuous change of lithium/carbon interaction energy, is related with the evacuation of mesopores where Li_n^+ clusters form meniscus. The mesopores are also responsible for an important irreversible capacity due to the easy access of solvated ions to the active surface where they are decomposed. Large hysteresis and irreversible capacity are two major drawbacks which preclude carbon nanotubes from any practical application in lithium-ion batteries.

Nanotubular carbon materials seem to be the most attractive for capacitor application especially after modifications, e.g., electrodeposition of a thin layer of conducting polypyrrole (PPy). Values of specific capacitance are markedly enhanced due to the contribution of pseudo-faradaic properties of PPy. The open entangled network of the nanocomposite favors the formation of a three dimensional electrical double layer in the bulk.

Amount of hydrogen reversibly stored at ambient conditions by electrodecomposition of water with a SWNTs electrode is below 0.5 wt%, that confirms recent investigations on these materials under a high pressure of dihydrogen. The very low micropore volume of nanotube materials seems to justify such a result. However, still a strict correlation between the nanostructural properties of nanotubes and the reversible capacity of hydrogen storage is missing and needs further elucidation. On the other hand, through this electrochemical process, absorption level on activated carbons is comparable to that of metallic alloys such as $LaNi_5$. Taking into account the extremely high cost of SWNTs and their poor performance, it is now more reasonable to study the relationship between the nanostructural parameters of activated carbon and their hydrogen storage capacity, in order to develop optimised materials for this process.

References

[1] Chau KT, Wong YS, Chan CC. An overview of energy sources for electric vehicles. Energy Conversion Manage 1999;40:1021–39.

[2] Buschow KHJ. In: Gschneidner KA, Eyring L, editors, Handbook on the physics and chemistry of rare earths, Hydrogen absorption in intermetallic compounds, vol. 6, New York: North Holland, 1984, pp. 1–111.

[3] Jurewicz K, Frackowiak E, Béguin F. Enhancement of reversible hydrogen capacity into activated carbon through water electrolysis. Electrochem Solid-State Lett 2001;4:A27–9.

[4] Smith W. The role of fuel cells in energy storage. J Power Sourc 2000;86:74–83.

[5] Aceves SM, Martinez-Frias J, Garcia-Villazana O. Analytical and experimental evaluation of insulated pressure vessels for cryogenic hydrogen storage. Int J Hyd Energy 2000;25:1075–85.

[6] Dresselhaus MS, Williams KA, Eklund PC. Hydrogen adsorption in carbon materials. MRS Bull 1999;24:45–50.

[7] Frackowiak E, Gautier S, Gaucher H, Bonnamy S, Béguin F. Electrochemical storage of lithium in multiwalled carbon nanotubes. Carbon 1999;37:61–9.

[8] Leroux F, Méténier K, Gautier S, Frackowiak E, Bonnamy S, Béguin F. Electrochemical insertion of lithium in catalytic multi-walled carbon nanotubes. J Power Sourc 1999;81–82:317–22.

[9] Wu GT, Wang CS, Zhang XB, Yang HS, Qi ZF, He PM, Li WZ. Structure and lithium insertion properties of carbon nanotubes. J Electrochem Soc 1999;146(5):1696–701.

[10] Béguin F, Méténier K, Pellenq R, Bonnamy S, Frackowiak E. Lithium insertion in carbon nanotubes. Mol Cryst Liq Cryst 2000;340:547–52.

[11] Gao B, Bower C, Lorentzen JD, Fleming L, Kleinhammes A, Tang XP, McNeil LE, Wu Y, Zhou O. Enhanced saturation lithium composition in ball-milled single-walled carbon nanotubes. Chem Phys Lett 2000;327:69–75.

[12] Claye AS, Fischer JE, Huffman CB, Rinzler AG, Smalley RE. Solid-state electrochemistry of the single wall carbon nanotube system. J Electrochem Soc 2000;147(8):2845–52.

[13] Niu C, Sichel EK, Hoch R, Moy D, Tennet H. High power electrochemical capacitors based on carbon nanotube electrodes. Appl Phys Lett 1997;70:1480–2.

[14] Frackowiak E, Méténier K, Bertagna V, Béguin F. Supercapacitor electrodes from multiwalled carbon nanotubes. Appl Phys Lett 2000;77:2421–3.

[15] Frackowiak E, Béguin F. Carbon materials for the electrochemical storage of energy in capacitors. Carbon 2001;39:937–50.

[16] Frackowiak E, Jurewicz K, Delpeux S, Béguin F. Nanotubular materials for supercapacitors. J Power Sourc 2001;97–98:822–5.

[17] Jurewicz K, Delpeux S, Bertagna V, Béguin F, Frackowiak E. Supercapacitors from nanotubes/polypyrrole composites. Chem Phys Lett 2001;347:36–40.

[18] Nützenadel C, Zuttel A, Chartouni D, Schlapbach L. Electrochemical storage of hydrogen in nanotube materials. Electrochem Solid-State Lett 1999;2(1):30–2.

[19] Rajalakshmi N, Dhathathreyan KS, Govindaraj A, Satishkumar BC. Electrochemical investigation of single-walled carbon nanotubes for hydrogen storage. Electrochim Acta 2000;45:4511–5.

[20] Che G, Lakshmi BB, Martin CR, Fisher ER. Metal-nanocluster-filled carbon nanotubes: catalytic properties and possible applications in electrochemical energy storage and production. Langmuir 1999;15:750–8.

[21] Britto PJ, Santhanam KSV, Rubio A, Alonso JA, Ajayan PM. Improved charge transfer at carbon nanotube electrodes. Adv Mater 1999;11:154–7.

[22] Hernadi K, Fonseca A, Nagy JB, Bernaerts D, Fudala A, Lucas AA. Catalytic synthesis of carbon nanotubes using zeolite support. Zeolite 1996;17:416–23.

[23] Hernadi K, Fonseca A, Piedigrosso P, Delvaux M, Nagy JB, Bernaerts D, Riga J. Carbon nanotubes production over Co/silica catalysts. Catal Lett 1997;48:229–38.

[24] Hamwi A, Alvergnat H, Bonnamy B, Béguin F. Fluorination of carbon nanotubes. Carbon 1997;35:723–8.

[25] Colomer JF, Piedigrosso P, Willems I, Journet C, Bernier P, Van Tendeloo G, Fonseca A, B'Nagy J. Purification of catalytically produced multi-wall nanotubes. J Chem Soc Faraday Trans 1998;94:3753–8.

[26] Kyotani T, Tsai L, Tomita A. Preparation of ultra fine carbon in nanochannels of an anodic aluminum oxide film. Chem Mater 1996;8:2109–13.

[27] Wakihara M, Yamamoto O, editors, Lithium ion batteries—fundamentals and performance, Tokyo, Weinheim: Kodansha, Wiley–VCH, 1998.

[28] Sawai K, Iwakoshi Y, Ohzuku T. Carbon materials for lithium-ion (shuttlecock) cells. Solid State Ionics 1994;69:273–83.

[29] Guérard D, Hérold A. Intercalation of lithium into graphite and other carbons. Carbon 1975;13:337–45.

[30] Béguin F. Cristallochimie de l'intercalation dans les formes cristallines du carbone. In: Bernier P, Lefrant S, editors, Le carbone dans tous ses états, Amsterdam: Gordon and Breach, 1997, pp. 405–55.

[31] Winter M, Besenhard JO, Spahr ME, Novak P. Insertion electrode materials for rechargeable lithium batteries. Adv Mater 1998;10:725–63.

[32] Chevallier F, Gautier S, Salvetat JP, Clinard C, Frackowiak E, Rouzaud JN, Béguin F. Effects of post-treatments on the performance of hard carbons in lithium cells. J Power Sourc 2001;97–98:143–5.

[33] Frackowiak E, Gautier S, Duclaux L, Méténier K, Béguin F. Role of microtexture and surface functionality of carbons used for lithium storage. ITE Battery Lett 1999;1(2):12–7.

[34] Winter M, Novak P, Monnier A. Graphites for lithium-ion cells: the correlation of the first-cycle charge loss with the Brunauer-Emmett-Teller surface area. J Electrochem Soc 1998;145(2):428–36.

[35] Duclaux L, Frackowiak E, Béguin F. Novel carbons from nanocomposites for high lithium storage. J Power Sourc 1999;81–82:323–7.

[36] Gautier S, Leroux F, Frackowiak E, Faugere MP, Rouzaud JN, Béguin F. Influence of the pyrolysis conditions on the nature of lithium inserted in hard carbons. J Phys Chem A 2001;105:5794–800.

[37] Orimo S, Majer G, Fukunaga T, Züttel A, Schlapbach L, Fujii H. Hydrogen in the mechanically prepared nanostructured graphite. Appl Phys Lett 1999;75:3093–5.

[38] Conway BE. In: Electrochemical supercapacitors–scientific fundamentals and technological applications, New York: Kluwer Academic/Plenum, 1999.

[39] Bunger U, Zuttel W. Hydrogen storage in carbon nanostructures — still a long road from science to commerce? Appl Phys A 2001;72:147–51.

[40] Carpetis C, Peschka W. A study on hydrogen storage by use of cryoadsorbents. Int J Hyd Energy 1980;5:539–54.

[41] Agarwal RK, Noh JS, Schwarz JA, Davini P. Effect of surface acidity of activated carbon on hydrogen storage. Carbon 1987;25:219–26.

[42] Dillon AC, Jones KM, Bekkedahl TA, Kiang CH, Bethune DS, Heben MJ. Storage of hydrogen in single-walled carbon nanotubes. Nature 1997;386:377–9.

[43] Ahn CC, Ye Y, Ratnakumar BV, Witham C, Bowman RC, Fultz B. Hydrogen desorption and adsorption measurements on graphite nanofibers. Appl Phys Lett 1998;73:3378–80.

[44] Lee SM, Park KS, Choi YC, Park YS, Bok JM, Bae DJ, Nahm KS, Choi YG, Yu SC, Kim N, Frauenheim T, Lee YH. Hydrogen adsorption and storage in carbon nanotubes. Synthetic Metals 2000;113:209–16.

[45] Liu C, Fan YY, Liu M, Cong HT, Cheng HM, Dresselhaus MS. Hydrogen storage in single-walled carbon nanotubes at room temperature. Science 1999;286:1127–9.

[46] Tibbetts GG, Meisner GP, Olk CH. Hydrogen storage capacity of carbon nanotubes, filaments, and vapor-grown carbon fibers. Carbon 2001;39:2291–301.

[47] Nützenadel C, Züttel A, Chartouni D, Schlapbach L. Electrochemical storage of hydrogen in nanotube materials. Electrochem Solid-State Lett 1999;2:30–2.

[48] Qin X, Gao XP, Liu H, Yuan HT, Yan DY, Gong WL, Song DY. Electrochemical hydrogen storage of multiwalled carbon nanotubes. Electrochem Solid-State Lett 2000;3:532–5.

[49] Nützenadel C, Züttel A, Schlapbach L. Electrochemical storage of hydrogen in carbon single wall nanotubes. In: Kuzmany H et al., editor, Electronic properties of novel materials-science and technology of molecular nanostructures, Melville, NY: American Institute of Physics, 1999, pp. 462–5.

[50] Rejalakshmi N, Dhathathreyan KS, Gowindraj A, Statishkumar BC. Electrochemical investigation of single-walled carbon nanotubes for hydrogen storage. Electrochim Acta 2000;45:4511–5.

[51] Ovshinsky SR, Fetcenko MA. Development of high catalytic activity disordered hydrogen-storage alloys for electrochemical application in nickel–metal hydride battery. Appl Phys A Mater Sci Process 2001;72(2):239–44.

[52] Jurewicz K, Frackowiak E, Fonseca A, Béguin F. Electrochemical reversible sorption of hydrogen into SWNTs. Chem Phys Lett 2001; submitted.